



Short-term mucosal disruption enables colibactin-producing *E. coli* to cause long-term perturbation of colonic homeostasis

Christine Harnack, Hilmar Berger, Lichao Liu, Hans-Joachim Mollenkopf, Till Strowig & Michael Sigal

To cite this article: Christine Harnack, Hilmar Berger, Lichao Liu, Hans-Joachim Mollenkopf, Till Strowig & Michael Sigal (2023) Short-term mucosal disruption enables colibactin-producing *E. coli* to cause long-term perturbation of colonic homeostasis, *Gut Microbes*, 15:1, 2233689, DOI: [10.1080/19490976.2023.2233689](https://doi.org/10.1080/19490976.2023.2233689)

To link to this article: <https://doi.org/10.1080/19490976.2023.2233689>



© 2023 The Author(s). Published with license by Taylor & Francis Group, LLC.



Published online: 10 Jul 2023.



Submit your article to this journal [↗](#)



View related articles [↗](#)



View Crossmark data [↗](#)

Short-term mucosal disruption enables colibactin-producing *E. coli* to cause long-term perturbation of colonic homeostasis

Christine Harnack^a, Hilmar Berger^a, Lichao Liu^a, Hans-Joachim Mollenkopf^b, Till Strowig^c, and Michael Sigal^{a,d}

^aDepartment of Gastroenterology and Hepatology, Charité - Universitätsmedizin, Berlin, Germany; ^bCore Facility Microarray, Genomics, Max Planck Institute for Infection Biology, Berlin, Germany; ^cDepartment of Microbial Immune Regulation, Helmholtz Centre for Infection Research, Braunschweig, Germany; ^dBerlin Institute for Medical Systems Biology, MDC Berlin, Berlin, Germany

ABSTRACT

Colibactin, a bacterial genotoxin produced by *E. coli* strains harboring the *pkS* genomic island, induces cytopathic effects, such as DNA breaks, cell cycle arrest, and apoptosis. Patients with inflammatory bowel diseases, such as ulcerative colitis, display changes in their microbiota with the expansion of *E. coli*. Whether and how colibactin affects the integrity of the colonic mucosa and whether *pkS+* *E. coli* contributes to the pathogenesis of colitis is not clear. Using a gnotobiotic mouse model, we show that under homeostatic conditions, *pkS+* *E. coli* do not directly interact with the epithelium or affect colonic integrity. However, upon short-term chemical disruption of mucosal integrity, *pkS+* *E. coli* gain direct access to the epithelium, causing epithelial injury and chronic colitis, while mice colonized with an isogenic $\Delta clbR$ mutant incapable of producing colibactin show a rapid recovery. *pkS+* *E. coli* colonized mice are unable to reestablish a functional barrier. In turn, *pkS+* *E. coli* remains in direct contact with the epithelium, perpetuating the process and triggering chronic mucosal inflammation that morphologically and transcriptionally resembles human ulcerative colitis. This state is characterized by impaired epithelial differentiation and high proliferative activity, which is associated with high levels of stromal R-spondin 3. Genetic overexpression of R-spondin 3 in colon myofibroblasts is sufficient to mimic barrier disruption and expansion of *E. coli*. Together, our data reveal that *pkS+* *E. coli* are pathobionts that promote severe injury and initiate a proinflammatory trajectory upon contact with the colonic epithelium, resulting in a chronic impairment of tissue integrity.

ARTICLE HISTORY

Received 5 April 2023
Revised 28 June 2023
Accepted 3 July 2023

Keywords



Inflammatory bowel diseases; colitis; microbiota; mucosal barrier; colibactin; *E. coli*; stem cells; regeneration

Introduction

Colibactin is a secondary metabolite that belongs to the group of cyclomodulins produced by *E. coli* of the phylogenetic group B2 and other gram-negative bacteria that carry the polyketide synthase (*pkS*) genomic island.¹ Such *pkS+* bacteria are found in about 20% of the Western population. Although they are considered commensals in the colonic flora, *pkS+* *E. coli* have gained considerable attention as potential drivers of colorectal carcinogenesis due to their genotoxic effects.^{2–7} Patients with inflammatory bowel disease (IBD), particularly those with ulcerative colitis, have high levels of *E. coli* in the gut.^{8,9} In particular, group B2 carriage has been found to be highly abundant in these patients.¹⁰ Accordingly, it has been proposed that a higher proportion of IBD patients carry *pkS+* *E. coli* than healthy individuals.²

Upon the direct attachment of *pkS+* bacteria to host cells, colibactin can cause DNA crosslinks, resulting in DNA double-strand breaks¹. Using organoids, we recently demonstrated that exposure to colibactin leads to the transformation of a subset of cells.⁴ However, most cells respond with cell cycle arrest, which results in megalocytosis, cellular senescence, and apoptosis.^{4,11} The relevance of these cytopathic effects on colonic epithelial homeostasis and function *in vivo* remains unclear. Moreover, whether *pkS+* *E. coli* contributes to the pathogenesis of colitis has not yet been investigated. As the colon epithelium is crucial for the maintenance of an efficient barrier, we hypothesized that colibactin's cytopathic effects have the potential to interfere with colonic tissue integrity, promote colonic crypt dysfunction, and cause colitis.

To address this, we developed a gnotobiotic *E. coli*-free mouse model. We successfully colonized these mice with the commensal *pkS+* M1/5 *E. coli*

CONTACT Michael Sigal  michael.sigal@charite.de  Department of Hepatology and Gastroenterology, Charité - Universitätsmedizin, Augustenburger Platz 1, Berlin 13353, Germany

© 2023 The Author(s). Published with license by Taylor & Francis Group, LLC.

This is an Open Access article distributed under the terms of the Creative Commons Attribution-NonCommercial License (<http://creativecommons.org/licenses/by-nc/4.0/>), which permits unrestricted non-commercial use, distribution, and reproduction in any medium, provided the original work is properly cited. The terms on which this article has been published allow the posting of the Accepted Manuscript in a repository by the author(s) or with their consent.

strain and found that colonization did not affect epithelial homeostasis. However, once mice experience a short-term chemical injury induced by dextran sulfate sodium (DSS), which transiently destroys the protective mucus barrier, *pks+* *E. coli* gain direct access to the epithelium. As a result, they increase the severity of colitis and render the mucosa incapable of restoring a functional barrier. This promotes chronic inflammation, causing a state that resembles human ulcerative colitis.

Results

Mucus barrier disruption facilitates colibactin-induced pathology

To study how colibactin-producing *E. coli* affects the colon epithelium, we first obtained and established an in-house colony of specific pathogen-free (SPF) *E. coli*-free mice, originally colonized with the Charles River altered Schaedler's flora (CRASF®).¹² Consistent with previous reports,^{13,14} our specific pathogen-free (SPF) mice appeared healthy and developed normally, showing no pathological behavior and exhibiting normal colon histology and weight when compared to mice with a conventional microbiota from our facility (Figure 1a,b).

After confirming that SPF mice did not harbor *E. coli*, we colonized them with a commensal M1/5 *E. coli* isolate, which efficiently expressed colibactin and induced cytopathic effects such as DNA damage and megalocytosis in cell lines and organoids.⁴ Mice were pretreated with streptomycin for 2 days and colonized with 1×10^9 colony-forming units (CFU) of M1/5 *E. coli*. CFU analysis using *E. coli*-specific MacConkey agar plates confirmed that all mice were successfully infected, whereas no *E. coli* was found in uninfected mice. *E. coli* colonization levels gradually decreased from an initial level of approximately 1×10^7 CFU/g feces to a plateau of approximately 1×10^6 CFU/g feces within 2 weeks (Figure 1c). The infection did not induce any phenotypic or weight changes in the mice, nor did it affect the epithelial morphology in the colon (Figure 1a,b).

Colibactin-expressing *E. coli* rely on direct interactions with the epithelium to exert their cytotoxic effects.⁸ We investigated whether such direct interactions occur *in vivo* under homeostatic conditions. Using fluorescence in situ hybridization (FISH) to

map the microbial distribution in the colon of mice infected with *pks+* *E. coli*, we found that a thick mucus layer separated the luminal microbiota from the healthy colonic epithelium, indicating that no interaction occurred between *E. coli* and gut epithelial cells (Figure 1d). Thus, we concluded that under healthy conditions, colibactin-producing *E. coli* are separated from the epithelium by mucus and do not affect colonic epithelial homeostasis.

We next investigated whether disruption of the mucus barrier enables *pks+* *E. coli* to gain access to the epithelium and affect homeostasis. To address this, SPF mice were infected with M1/5 *E. coli* as described above, and then treated with a single 7-day cycle of DSS, starting at day 5 post-infection (Figure 1e). DSS is a sulfated sugar that disrupts mucus and causes colonic mucosal injury.¹⁵ FISH analysis of the colon after five days of DSS treatment showed disruption of the mucus layer, with the microbiota in direct contact with the colonic epithelium (Figure 1g). Moreover, *E. coli* CFU analysis revealed that DSS treatment caused *E. coli* expansion (Figure 1f). While control SPF mice treated with DSS without prior colonization with *E. coli* showed only mild weight loss in response to DSS, mice colonized with *pks+* *E. coli* showed significantly greater weight loss and delayed weight gain once DSS was discontinued (Figure 1h).

To address whether this effect is driven by colibactin itself, we repeated the experiment and infected the animals with either WT M1/5 *E. coli* or the $\Delta clbR$ isogenic mutant, which lacks *clbR*, a key transcriptional regulator of colibactin production.¹⁶ In contrast to the mice infected with the WT M1/5 strain, mice infected with the $\Delta clbR$ mutant lost almost no weight in response to DSS treatment (Figure 1i).

Together, these data indicate that DSS-induced disruption of the mucus barrier enables microbes to gain direct access to the colon epithelium, leading to the expansion of resident *E. coli*. Under these conditions, colibactin expression is associated with severe weight loss in mice.

Colibactin enhances mucosal injury upon DSS treatment

As our data indicate that colibactin causes weight loss upon DSS treatment, we investigated its effect on the colon epithelium. For this, we infected animals with

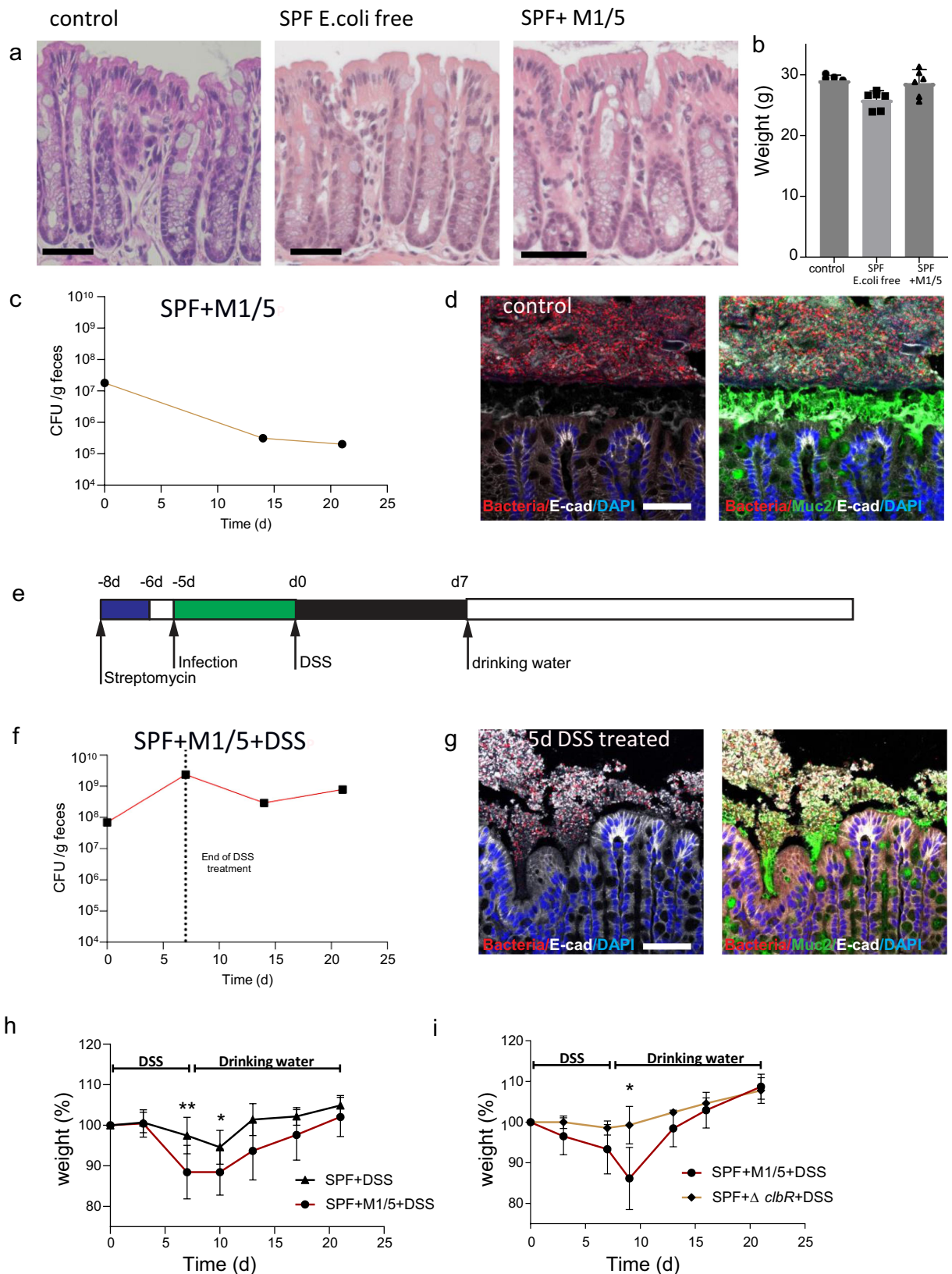


Figure 1. Colibactin exacerbates DSS-induced colitis. (a) H&E staining of colon tissue from a control mouse, an SPF E. coli-free mouse, and an SPF mouse colonized with the *pks+* M1/5 E. coli strain (scale bars: 50 μ m). (b) Weight of the three groups shown in A ($n = 6$ mice per group). (c) Colonization levels with M1/5 E. coli over time ($n = 9$ mice). (d) Fluorescence in situ hybridization (FISH) for bacteria (general EUB338 probe, red) in sections of control mice showed no interaction between bacteria and the epithelium, as they were separated by a thick mucus layer (scale bar 50 μ m). (e) Treatment schematic for infection of SPF E. coli-free mice with WT M1/5 E.

WT or $\Delta clbR$ M1/5 and sacrificed them immediately after DSS treatment (Figure 2a). Spatial mapping of mucus thickness and microbial distribution in the colon using FISH revealed that both WT and $\Delta clbR$ infected animals experienced a disruption of the mucus layer upon DSS treatment, allowing direct interaction between microbes and surface epithelial cells (Figure 2b). Thus, we concluded that DSS promoted barrier disruption independently of colibactin. CFU analysis demonstrated high levels of *E. coli* colonization in both of the groups (Figure 2b, right panel). However, morphological analysis of the colon tissue using H&E staining showed that injury was significantly more extensive in mice infected with WT M1/5 *E. coli* compared to the mutant. Mice infected with WT *E. coli* had a significantly larger proportion of injured crypts, characterized by disruption of the crypt structure with only a thin remaining cell layer covering the mucosa or full lack of epithelium (ulcer formation) (Figure 2c). Moreover, the analysis of crypt height in the remaining crypts showed a more severe reduction in the WT M1/5 group (Figure 2d). As colibactin has been reported to induce DNA double-strand breaks in primary epithelial cells, leading to senescence and cell death, we next analyzed the direct effects of colibactin on colon epithelial cells in our mice. Immunolabelling for γ H2AX, which detects cells with DNA breaks and marks the initiation of DNA repair, revealed an increased number of γ H2AX+ cells in mice colonized with WT M1/5 compared with the $\Delta clbR$ mutant (Figure 2e). Taken together, we conclude that upon disruption of the mucus barrier, colibactin promotes DNA damage and extensive injury to the colon epithelium.

***pks+* E. coli locks the mucosa in a chronic regenerative state**

Next, we repeated the experiment but sacrificed the animals 7 days after DSS withdrawal to examine how recovery was affected by the presence of

colibactin (Figure 3a). At this time point, mice infected with $\Delta clbR$ *E. coli* showed an almost completely restored mucus barrier, whereas in animals infected with WT *E. coli* the barrier remained inefficient, and bacteria were still able to make contact with the epithelium (Figure 3b).

Histological analysis further revealed that crypt architecture in $\Delta clbR$ -infected animals appeared healthy, whereas WT-infected mice had elongated, polymorphic, distorted crypts with an increased number of proliferating cells marked by the expression of Ki67 (Figure 3c,d). Thus, we concluded that $\Delta clbR$ *E. coli*-infected mice were able to reestablish homeostasis within one week of DSS treatment, while WT-infected animals remained in a regenerative state, characterized by increased proliferation and an inefficient barrier function. Consistent with the lack of a mucus barrier, labeling for γ H2AX showed that WT-infected, but not $\Delta clbR$ -infected, mice still contained a large number of positive cells, indicating that colibactin-mediated DNA damage continues in this state.

To test whether recovery in the presence of *pks+* *E. coli* was achieved at a later time point, we treated infected animals with one cycle of DSS and allowed them to recover for 4 weeks. Even at this late time point, WT-infected mice still exhibited more severe barrier disruption, increased proliferation, and higher numbers of γ H2AX+ cells than $\Delta clbR$ -infected mice (Figure 3b–e, right panels).

Thus, we concluded that colibactin impairs epithelial recovery after injury and promotes a chronic regenerative state characterized by an inefficient mucus barrier and continued epithelial cell damage.

***pks+* E. coli-infected mice post-DSS develop chronic inflammation that resembles ulcerative colitis**

To investigate the mucosal response to colibactin in more detail, we performed transcriptome analysis of the colon tissue of WT- and $\Delta clbR$ -infected animals at 4 weeks post-DSS.

coli or $\Delta clbR$ mutant. (f) Levels of M1/5 *E. coli* over time after DSS treatment ($n = 9$ mice). Colitis leads to an increase in the bacterial number, which remains stable during regeneration. (g) FISH for bacteria (general EUB338 probe, red) co-stained with E-cadherin (white) and Muc2 (green) in sections from mice treated with DSS for 5 d with DSS. The mucus layer is broken down, and bacteria can be found in close proximity to the epithelium (scale bar 50 μ m). (h) Weight curves of uninfected mice ($n = 8$) and M1/5 *E. coli*-infected SPF mice ($n = 13$) during DSS treatment and recovery. (i) Weight curves of WT M1/5 *E. coli*-infected SPF mice ($n = 5$) and $\Delta clbR$ mutant-infected SPF mice ($n = 4$) during DSS treatment and regeneration *: $p < 0.05$, **: $p < 0.01$ calculated by Student's t-test. All data are presented as mean \pm SD.

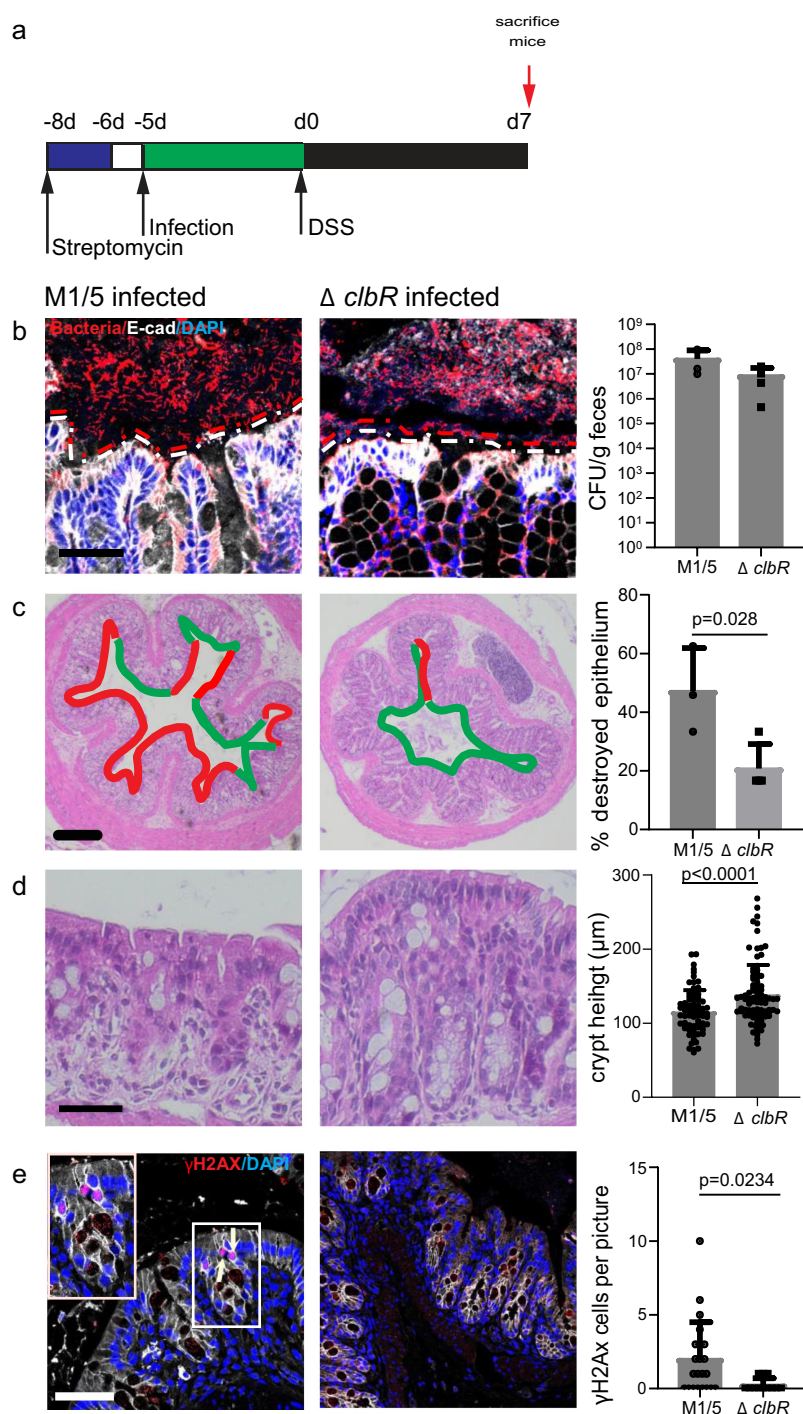


Figure 2. Colibactin increases the severity of tissue damage after DSS. (a) Treatment schematic for infection of SPF mice with WT M1/5 *E. coli* or Δ *clbR* mutant. (b) Left: FISH for bacteria (general EUB338 probe, red) in colon sections from SPF mice infected with WT M1/5 *E. coli* or Δ *clbR* mutant (white line indicates epithelial lining, red line indicates border of intestinal microbiota in proximity to the epithelial surface). Right: *E. coli* colonization levels on day 7 of DSS treatment (WT, $n = 3$ mice; Δ *clbR* $n = 4$ mice). (c) H&E staining of colon sections from SPF mice infected with M1/5 *E. coli* or Δ *clbR* mutant. Red lines indicate injured tissue, green lines indicate epithelial lining that remains intact. Right: Quantification of the proportion of disrupted epithelium. (d) Colon crypt height of SPF mice infected with M1/5 *E. coli* or Δ *clbR* mutant (WT $n = 3$ mice, Δ *clbR* $n = 4$ mice). (e) Confocal microscopy images of colon tissue from SPF mice infected with M1/5 *E. coli* or the Δ *clbR* mutant on d 7 of DSS treatment stained for γ H2AX (red) and DAPI, indicating more DNA damage (white arrows) in WT M1/5 *E. coli*-infected mice. Right: quantification of γ H2AX-positive cells (WT, $n = 3$ mice; Δ *clbR* $n = 4$ mice). P-values were calculated using Student's t-test. All data are presented as mean \pm SD.

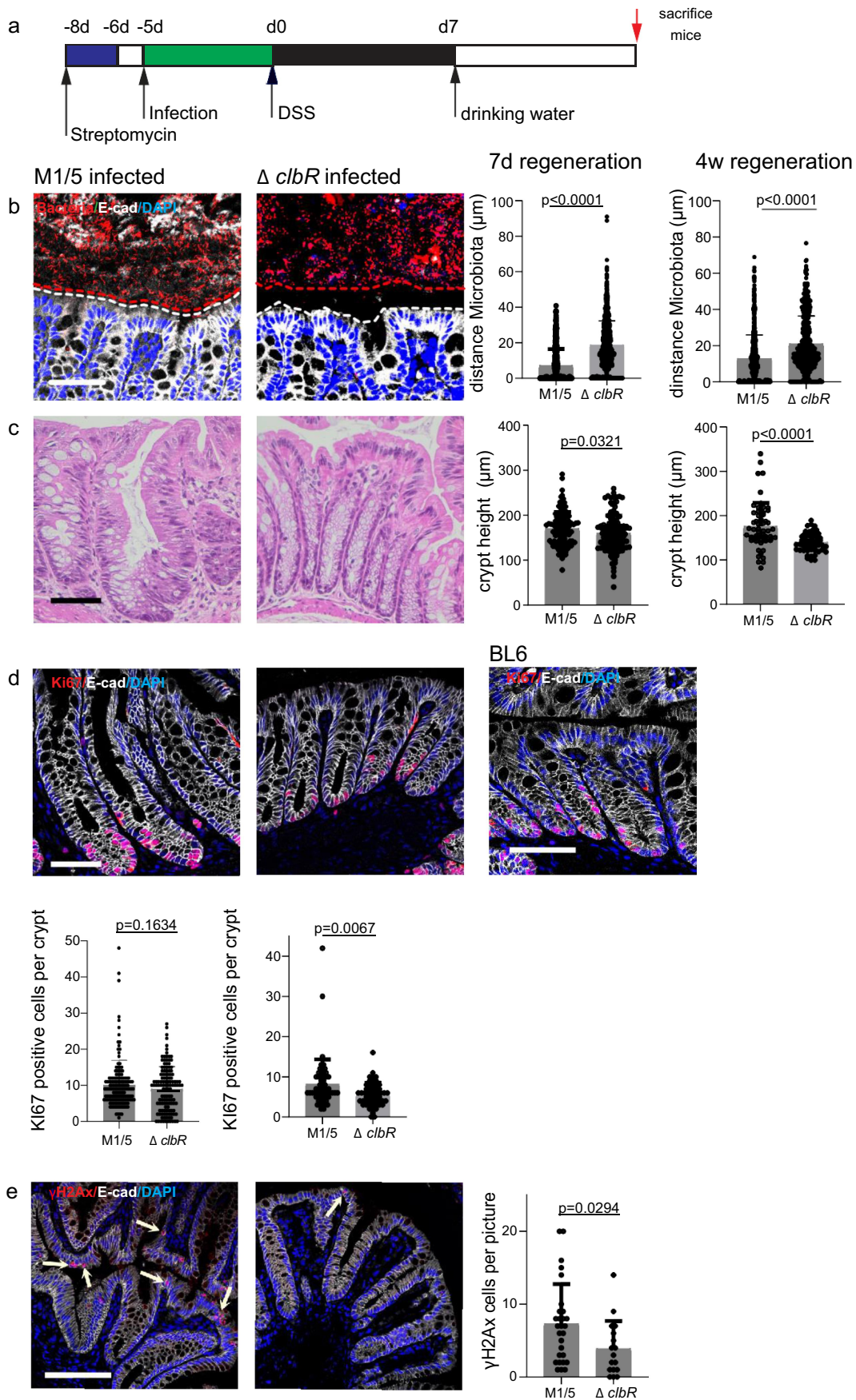


Figure 3. Colibactin delays tissue regeneration upon injury. (a) Treatment schematic for infection of SPF mice with WT M1/5 *E. coli* or $\Delta clbR$ mutant. (b) FISH for bacteria (general EUB338 probe, red) in colon sections of SPF mice infected with WT M1/5 *E. coli* or the $\Delta clbR$ mutant (white line indicates epithelial lining, red line indicates border of intestinal microbiota in proximity to the epithelial

We observed that many of the most highly regulated genes were associated with inflammation. Chronic colonic inflammation is a key feature of ulcerative colitis (UC). We asked whether the transcriptional alterations in our mice displayed similarities to the changes observed in patients with ulcerative colitis. Based on previously published transcriptome data from ulcerative colitis patients,¹⁷ we generated an ulcerative colitis signature gene set and performed gene set enrichment analysis (GSEA). Indeed, transcriptome data from our mice revealed a significant positive enrichment of genes upregulated in ulcerative colitis, as well as a significant negative enrichment of genes downregulated in ulcerative colitis¹⁷ (Figure 4a). We investigated which colitis-associated genes were upregulated in our WT M1/5-infected mice and found that many of these genes were involved in critical immune signaling pathways, such as IL-1/NF- κ B and IL-6 (Figure 4b). We next performed immunofluorescence labeling of colon tissues from mice at 4 weeks post-DSS for immune cell markers and found a significantly higher immune cell infiltration in WT M1/5 *E. coli*-colonized mice than in the Δ *clbR*-colonized animals, reflected by higher levels of CD3, IBA1, and MPO (Figure 4c). Thus, we conclude that colibactin triggers mucosal inflammation that transcriptionally overlaps with changes observed in ulcerative colitis.

The mucosa in ulcerative colitis is characterized by an up-regulation of regenerative signals that enhance proliferation and inhibit differentiation

Since we found that colibactin triggered an increased proliferation of epithelial cells, we asked whether similar responses were also observed in ulcerative colitis. We obtained tissue from patients with ulcerative colitis who underwent colon

surgery as well as samples of healthy mucosa from patients who underwent colon surgery for other reasons. Histological analysis and labeling for Ki67 revealed a highly proliferative, regenerative epithelium in colitis patients compared to that in healthy controls (Figure 5a). By further investigating which of the genes that were upregulated in both our M1/5 *E. coli* colonized mice and ulcerative colitis patients could promote increased proliferative activity, we identified several Wnt target genes, such as CD44 and MMP7, which are known to be expressed in colonic stem and progenitor cells (Figure 5b). When we analyzed genes that were downregulated in both datasets, we found several genes expressed in differentiated enterocytes: there was a loss of key enterocyte markers such as Aqp8, Car4, and Vil1, as well as PPAR- γ , a key gene involved in the regulation of short-chain fatty acid metabolism in enterocytes (Figure 5b). Since enterocyte differentiation and the expression of the aforementioned genes are known to be negatively affected by Wnt signaling,¹⁸ we searched for a regulator that could drive increased Wnt signaling. Stroma-derived R-spondin 3 has been shown to be a critical determinant of Wnt signaling and epithelial regeneration in the colon and is increased in the context of injury.^{19,20} We noticed that in the published transcriptome dataset the expression of R-spondin 3 was significantly higher in ulcerative colitis samples than in healthy controls (Figure 5b). RNA in situ hybridization in human samples confirmed high expression of R-spondin 3 in the stroma of ulcerative colitis patients (Figure 5c). Similarly, post-DSS we found increased expression of R-spondin 3 in the stroma of mice colonized with WT M1/5 *E. coli* compared to mice colonized with the Δ *clbR* mutant (Figure 5c, right). Using qPCR of murine colon tissue, we confirmed that compared to mice infected with the Δ *clbR* mutant strain, mice colonized with WT *E. coli* expressed

surface). Right: quantification of the distance between the epithelium and the microbiota after 7 d (WT, $n = 3$ mice; Δ *clbR* $n = 3$ mice) and 4 weeks (WT $n = 3$ mice, Δ *clbR* $n = 3$ mice). (c) H&E staining of the colon of SPF mice infected with WT M1/5 *E. coli* or Δ *clbR* mutant. Right: quantification of crypt height after 7 days (WT, $n = 7$ mice; Δ *clbR* $n = 6$ mice) and 4 weeks (WT $n = 3$ mice, Δ *clbR* $n = 3$ mice). (d) Confocal microscopy images of colon tissue from SPF mice infected with WT M1/5 *E. coli* or the Δ *clbR* mutant on day 7 of regeneration, stained for Ki67 (red), E-cadherin (white), and DAPI. Right: Quantification of Ki67-positive cells per crypt after 7 days (WT, $n = 7$ mice; Δ *clbR* $n = 6$ mice) and 4 weeks (WT, $n = 3$ mice; Δ *clbR* $n = 3$ mice). (e) Confocal microscopy images of colon tissue from SPF mice infected with WT M1/5 *E. coli* or the Δ *clbR* mutant on day 7 of regeneration stained for γ H2AX (red, as shown by arrows) E-cadherin (white) and DAPI. Right: Quantification of γ H2AX-positive cells per image. P-values were calculated using Student's t-test. All data represent mean \pm SD

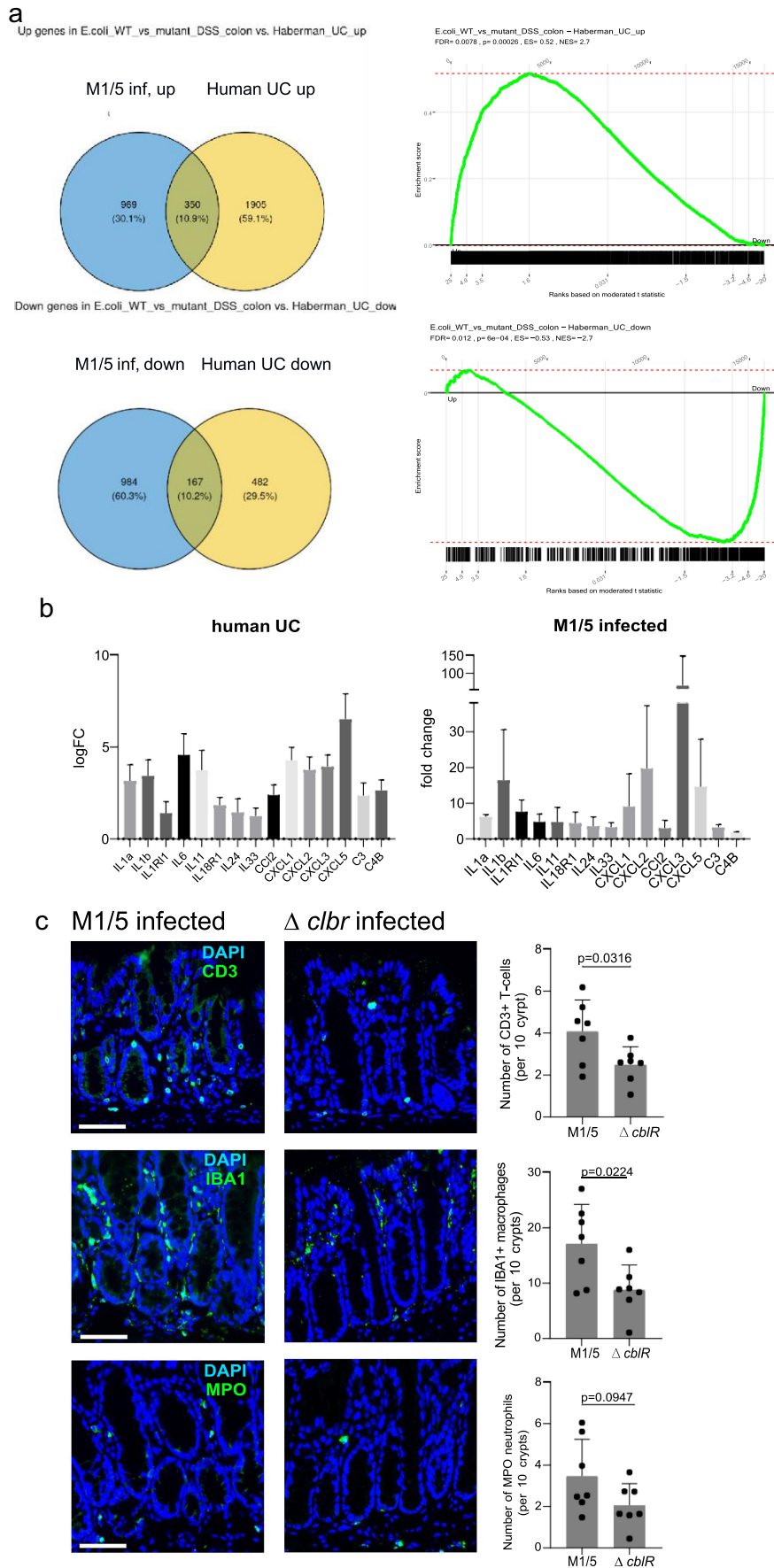


Figure 4. Infection with *pkS+* *E. coli* causes inflammation that resembles ulcerative colitis. (a) Venn diagrams of genes upregulated (top) and downregulated (bottom) in human ulcerative colitis patients compared with genes upregulated or downregulated in mice infected with WT M1/5 *E. coli* vs. the Δ *cbIR* mutant. GSEA showed an overlap between the regulated genes in human patients and WT

increased levels of R-spondin 3 and its receptor Lgr5, which is itself a WNT/R-spondin target gene. In contrast, the enterocyte markers Aqp8 and Car4 were significantly downregulated (Figure 5d). Together, these data revealed increased Wnt signaling in mice colonized with M1/5 *E. coli*, which depends on the presence of colibactin. This is associated with increased proliferation and loss of enterocyte differentiation. All these features were also found in the colonic mucosa of patients with ulcerative colitis.

Increased R-spondin 3 expression promotes proliferation but reduces barrier integrity

To investigate whether R-spondin/Wnt signaling contributes to the mucosal responses observed in our mice, we utilized *Myh11-CreERT2/Rosa26Sor*⁶ (CAG - Rspo3) mice, which conditionally overexpress R-spondin 3 in stromal Myh11+ myofibroblasts upon administration of tamoxifen, in order to mimic the overexpression observed in WT M1/5 *E. coli* infected mice. Mice were sacrificed 14 days after tamoxifen treatment.

H&E staining revealed marked crypt elongation, which was associated with increased expression of Ki67, as detected by immunofluorescence labeling (Figure 6a–d). When we performed transcriptome analysis of colon tissue from WT and R-spondin 3 KI mice, we found significant upregulation of R-spondin 3, Lgr5, and MMP7 (Figure 6e), all of which were also upregulated in WT M1/5-colonized mice post-DSS (see Figure 5b). Myc, another central target of Wnt/R-spondin, was also upregulated. Similarly, there was a significant downregulation of the key enterocyte markers Aqp8 and Car4.

To address how this affects the mucosal barrier, we performed ISH to visualize the microbiota and found that overexpression of R-spondin 3 was sufficient to promote loss of the barrier, allowing direct interaction of bacteria with the epithelium (Figure 6f,g).

CFU analysis of *E. coli* in R-spondin 3 KI mice and their corresponding WT littermates at 14 days after tamoxifen treatment also confirmed a significant increase in *E. coli* colonization upon R-spondin 3 overexpression (Figure 6h).

Together, these data show that increased regeneration driven by the stem cell niche occurs at the expense of differentiation, resulting in a loss of mature cell types, insufficient barrier function, and dysbiosis characterized by an expansion of *E. coli*.

Overall, our data reveal a new concept of how transient disruption of the mucosal barrier can enable a powerful toxin expressed by a common member of the microbiota to initiate a long-term disruption of tissue integrity, promote a proinflammatory trajectory, and contribute to chronic colitis.

Discussion

Here, we revealed a mechanism by which colibactin-expressing *E. coli* can contribute to the chronification of acute experimental colitis. The resulting epithelial pathology closely resembles that of human ulcerative colitis, suggesting that this common human pathobiont can play a causative role in the development of the disease.

Crucially, the double-hit mechanism we identified explains why carriers of *pks+* bacteria do not necessarily develop disease: during homeostatic conditions, the mucus barrier of the colon prevents the bacteria from reaching the epithelial cells. Only a second hit that causes mucus barrier breakdown enables bacteria to make direct contact, which in turn unleashes the full toxic potential of colibactin. Thus, we hypothesize that although *pks+* *E. coli* are harmless to the healthy colonic mucosa, carriers are at an elevated risk of developing chronic epithelial dysfunction in the wake of an unrelated colonic injury. This would explain their overrepresentation among ulcerative colitis patients.

We have previously shown that damage to the colonic mucosa leads to the reversal of cellular

M1/5 *E. coli*-infected mice. (b) Bar charts of fold-change of inflammatory genes upregulated in published transcriptome data from human ulcerative colitis patients¹² (left) and mice infected with WT M1/5 *E. coli* (right), as assessed by microarray analysis. (c) Confocal microscopy images of colon tissue from SPF mice infected with WT M1/5 *E. coli* or the Δ cIbR mutant after four weeks of regeneration stained for CD3 (green), IBA1 (green), and MPO (green) co-stained with DAPI ($n = 3$ mice per group).

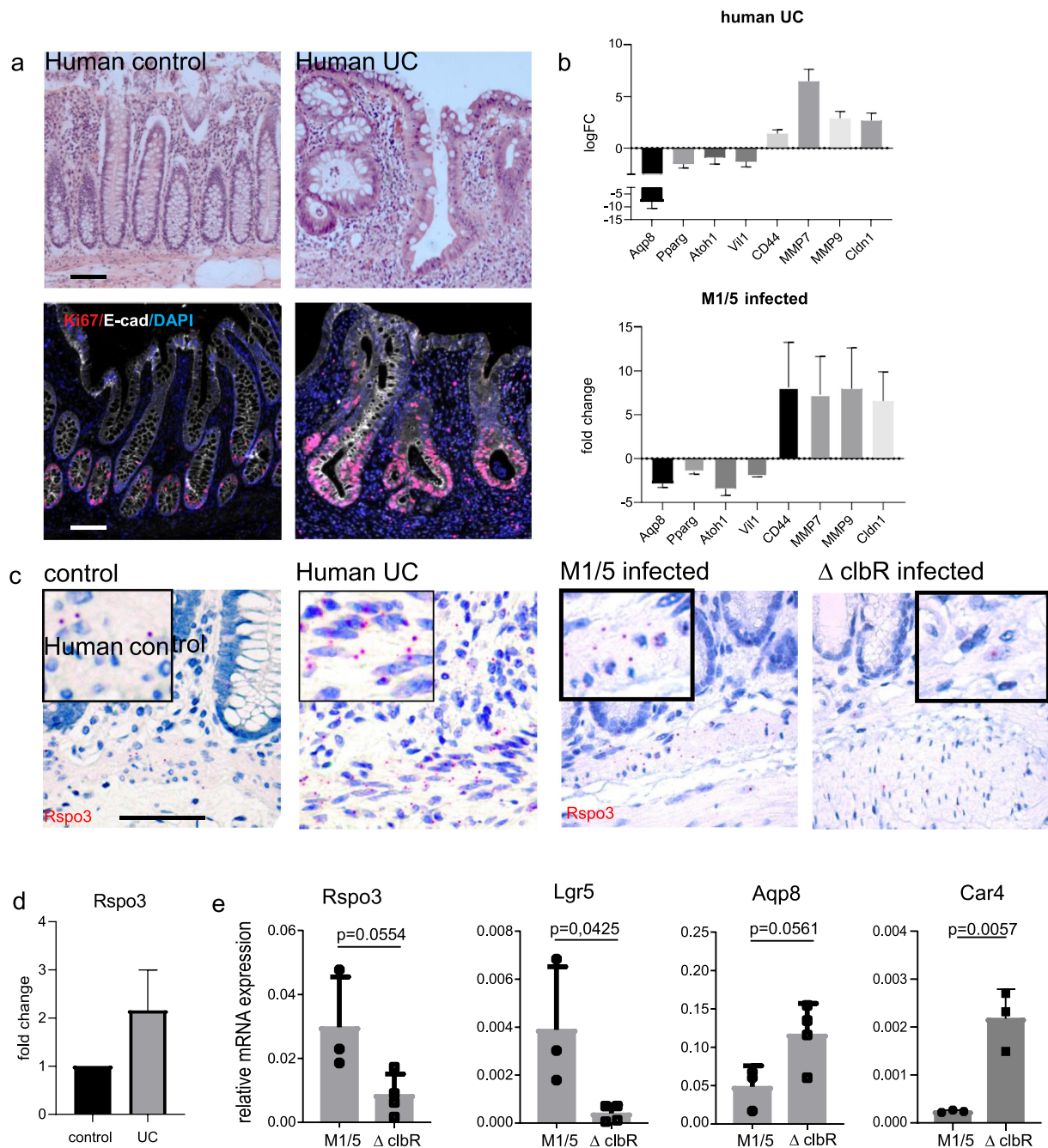


Figure 5. Epithelial changes seen in mice infected with WT M1/5 *E. coli* resemble those of human ulcerative colitis. (a) Human colon tissue without colitis and during active ulcerative colitis stained with H&E (top) and imaged by confocal microscopy (bottom) stained with Ki67 (red), E-cadherin (white), and DAPI. (b) Fold-changes in epithelial genes regulated in human ulcerative colitis¹² and SPF mice infected with WT M1/5 *E. coli* as measured by microarray. (c) Microscopic images of single-molecule ISH for R-spondin 3 in human colon tissue without colitis and during active ulcerative colitis, as well as colon tissue from SPF mice infected with WT M1/5 *E. coli* or the Δ clbR mutant after 4 weeks of regeneration post-DSS. (d) Quantification of R-spondin 3 expression in human colon tissue without colitis and during active ulcerative colitis (data extracted from Habermann et al.) (e) qPCR for *Rspo3*, *Lgr5*, *Aqp8* (WT $n = 3$ mice, Δ clbR $n = 4$ mice for all three genes), and *Car4* (WT $n = 3$ mice, Δ clbR $n = 3$ mice) of RNA from SPF mice infected with WT M1/5 *E. coli* or the Δ clbR mutant after 1 month of regeneration after DSS treatment. P-values were calculated using Student's t-test. Data represent mean \pm SD

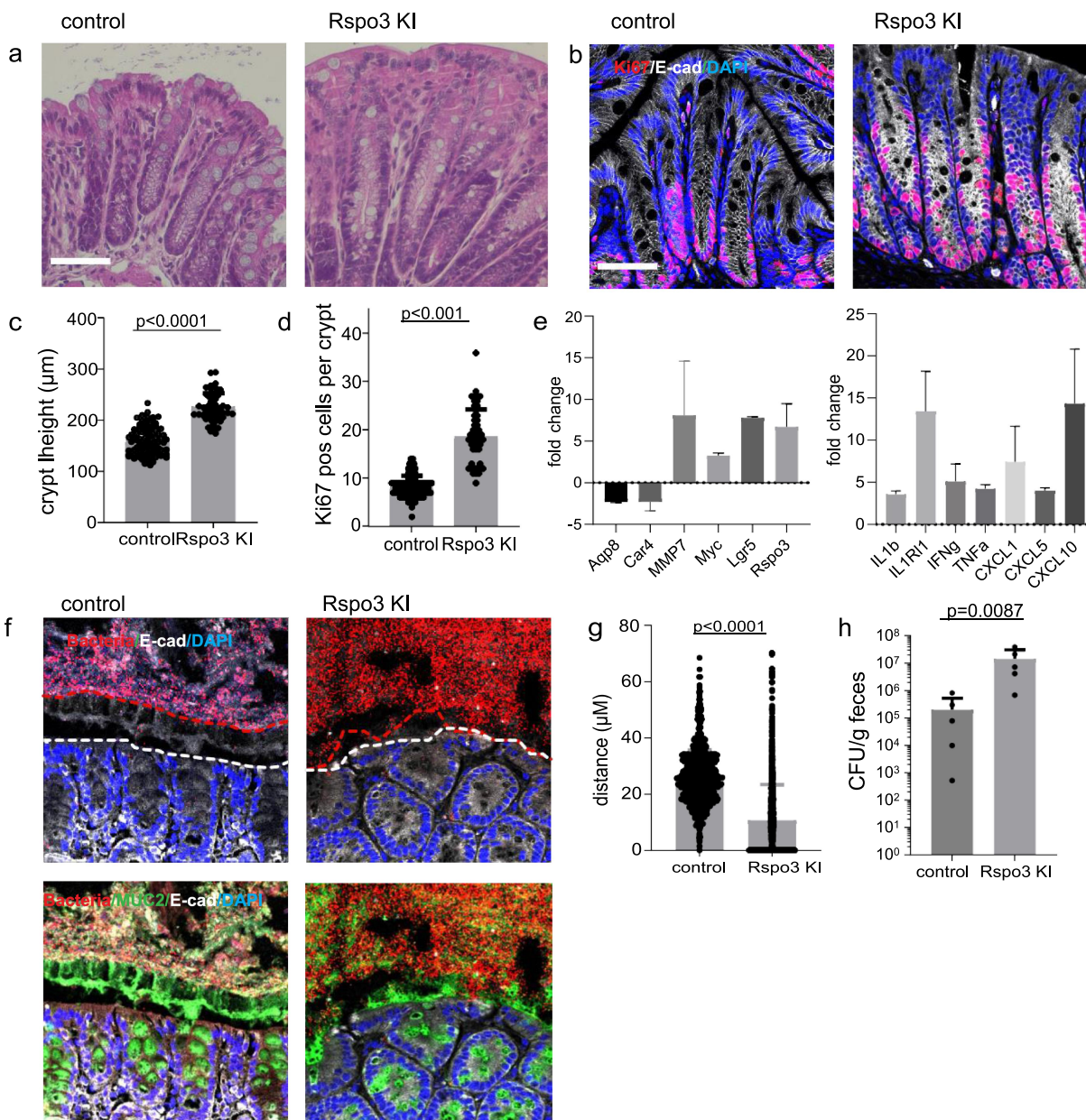


Figure 6. R-spondin 3 overexpression is sufficient to disrupt the mucosal barrier. (a) H&E staining of colon tissue from control and Rspo3 KI mice 14 days after tamoxifen treatment (b) Confocal microscopy images of colon tissue from control and Rspo3 KI mice 14 days after tamoxifen treatment stained for Ki67 (red), E-cadherin (green), and DAPI. (c) Quantification of crypt length in colon tissue from control ($n = 4$) and Rspo3 KI ($n = 4$) mice 14 days after tamoxifen treatment. (d) Quantification of Ki67+ cells per crypt section in control ($n = 4$) and Rspo3 KI mice ($n = 4$) 14 days after tamoxifen treatment. (e) Fold-changes in regulated epithelial genes in Rspo3 KI mice compared to control mice as assessed by microarray. (f) Fluorescence in situ hybridization for bacteria (general EUB338 probe, red) in sections of control and Rspo3 KI mice 14 days after tamoxifen treatment (white line indicates epithelial lining, red line indicates the border of intestinal microbiota in proximity to the epithelial surface). (g) Quantification of the distance between the microbiota and epithelium in control and Rspo3 KI mice ($n = 3$ mice per group) (h) *E. coli* colonization levels in control and Rspo3 KI mice (mice with “conventional microbiota” were used and quantitative plating for *E. coli* in the stool performed). P-values were calculated using Student’s t-test. All data represent mean \pm SD

hierarchy, including loss of resident stem cells and reprogramming of colonocytes into rapidly proliferating stem cells that give rise to new crypts.¹⁹ This regenerative state comes at a cost: mature cells are

lost, leaving the mucosa temporarily unprotected by a mucous barrier until mature crypts have been regenerated. Our findings in mice colonized with the mutant *E. coli* strain show that in the absence

of colibactin, this regeneration process is rapid and effectively prevents major weight loss in animals. In our model, colibactin thus served as the key factor that induced cell damage and prevented homeostasis from being reestablished. Our data do not allow any conclusions to be drawn on whether colibactin actively promotes the regenerative state or whether it causes severe cell damage through which the epithelium is continually eroded. The recognition that cellular identities are not fixed and that epithelial regeneration involves the breakdown of cellular hierarchy, reprogramming of differentiated cells, and their recruitment into the stem cell pool is relatively recent.²¹ Therefore, we have as yet no good understanding of what signals trigger the induction of the regenerative state or control the reestablishment of normal homeostasis with fully differentiated cells.

Chronic inflammatory diseases, such as Crohn's disease or ulcerative colitis, are characterized by impaired barrier function.²² This barrier is maintained by various short-lived differentiated cells, which are constantly replenished by Lgr5+ stem cells situated in the crypt base.^{23,24} Secretory goblet cells produce mucus, which is important for the maintenance of the antimicrobial barrier.²⁵ In addition, enterocytes control the microbiota in various ways: they produce antimicrobial proteins and their metabolism is important for maintaining homeostasis between the epithelium and the microbiota.^{18,26} Colonocytes rely on short-chain fatty acids produced by the anaerobic flora and their metabolism via beta-oxidation. This in turn creates an anaerobic milieu in the colon, which is essential for the maintenance of anaerobic bacteria.²⁷ In the context of injury and inflammation, this symbiotic cross-talk is disrupted and oxygen levels in the lumen increase, leading to a loss of anaerobes and a selective advantage for facultative anaerobes, such as *E. coli*. In congruence with this, we found overgrowth of *E. coli* following DSS-induced damage.

Several clinically relevant enteropathogens are facultative anaerobes, e.g. *Salmonella*, *Citrobacter* and pathogenic *E. coli*. Interestingly, *Salmonella* and *Citrobacter* have evolved to actively induce increased oxygen levels in the colon, which facilitates their expansion²⁸ – suggesting that colibactin carriage may be similarly adaptive to *E. coli*.

Interestingly, *Citrobacter* causes increased oxygen levels by inducing hyperplasia and an increase in proliferating cells via massively increasing R-spondin levels.²⁹ In congruence, we found that when hyperplasia was genetically induced by overexpression of R-spondin 3, this was accompanied by overgrowth of *E. coli* and barrier loss. In contrast to enteropathogens, *pks+* *E. coli* do not appear to actively disrupt mucosal homeostasis. Instead, they require a “first hit” that damages the mucosal barrier and enables them to make direct contact with the epithelium. Potentially, such a first hit could be initiated by sporadic factors other than DSS: As well as chemical injuries triggered by transient infections and intoxications, the mucus barrier can also be affected by dietary or pharmacological interventions. A defective mucus barrier can also have genetic causes. For example, a number of known genetic risk factors for ileal Crohn's disease act by impairing the ability of Paneth cells to secrete the full complement of antimicrobial peptides that help to keep the mucus sterile and prevent bacteria from invading the crypts.³⁰

Similarly, the “second hit” that leads to chronicification may be caused by factors other than *pks+* *E. coli*. Indeed, *Klebsiella* and some other *Enterobacteriaceae* have been shown to carry *pks*. They, too, are facultative anaerobes that are likely to thrive close to the regenerative epithelium. In addition, other bacterial toxins from the microbiota may potentially be able to cause similarly severe damage when in direct contact with the epithelial cells. The findings in our knock-in mice also show that elevated R-spondin 3 levels themselves are sufficient to induce a regenerative state, barrier loss, and overgrowth of *E. coli*. Thus, targeting pathways that promote R-spondin 3 upregulation in chronic injury may represent a strategy to disrupt the vicious circle of injury, regeneration and dysbiosis. Indeed, a recent paper suggests that inhibition of IL-1 signaling may prevent the upregulation of R-spondin in the colon after injury.³¹

Overall, our results provide an important new perspective for understanding the etiology of ulcerative colitis. They show that the microbiota composition in experimental colitis models can have a direct and profound effect on the outcome. While this is already well appreciated at the species

level, we demonstrate that it is not sufficient to consider specific microbiota species, but that the carriage of pathogenicity determinants may be an even more important predictor of experimental outcomes.

Our double-hit model also points to new potential therapeutic targets for ulcerative colitis. All current therapy options target the immune response but usually fail to achieve complete remission. Approaches that target the toxic bacteria themselves may be able to remove the main driver of the disease, while monitoring for *pks* carriage could help identify susceptible individuals for preventative approaches, including lifestyle and eradication. In addition, dampening R-spondin 3 levels may restore the balance between epithelial proliferation and differentiation signals, allowing full maturation of surface cells and reestablishment of an effective barrier.

Methods

Mouse experiments

All procedures involving animals were approved by institutional and legal authorities (LaGeSo Berlin). All animals were maintained in autoclaved micro-isolator cages and provided with sterile drinking water and chow ad libitum. Male 6–8 week-old mice were used in this study.

To study how colibactin-producing *E. coli* affects the colon epithelium, we first obtained SPF *E. coli*-free mice that were originally colonized by the Charles River altered Schaedler flora (CRASF[®]). *E. coli*-free Bl6 mice were provided by Till Strowig. These mice were used to establish in-house colonies of Enterobacteriaceae-free C57BL/6 mice. The absence of *E. coli* was controlled by plating feces on MacConkey agar plates.

Human material

Human samples from patients with ulcerative colitis or healthy control tissue (from patients who underwent colon surgery for other reasons and where adjacent healthy tissue was available) were kindly provided by the Department of Pathology. The samples were de-identified, and the experiments were approved by the local ethics committee.

E. coli cultivation

M1/5 *E. coli*, a *pks*⁺ *E. coli* strain, and its isogenic $\Delta clbR$ mutant were provided by Ulrich Dobrindt and have been described previously.⁴ In the mutant strain, the *clbR* gene of the *pks* island was deleted, which prevented the synthesis of colibactin. Both strains carry a *rpsL* K42R mutation conferring streptomycin resistance. *E. coli* was cultured overnight at 37°C and 180 rpm in liquid LB Medium and diluted 1:33 in infection medium consisting of DMEM (Gibco), 10% FCS (Biochrom) the next day. The bacteria were allowed to grow to an OD600 of 1. Mice were infected with 1×10^9 CFU) via oral gavage. The required volume of bacterial suspension was centrifuged, and the density was adjusted to a concentration of 1×10^9 bacteria per 100 μ l of the infection medium.

Murine Infection

Enterobacteriaceae-free C57BL/6 mice were treated for 48 h with 2 mg/ml streptomycin in drinking water. Streptomycin was replaced with drinking water 24 h before infection. The mice were infected as described above. At 5 days post-infection, mice were treated with 2.5% DSS (MP Biomedical, 36000–50,000 MW, CAS number 9011-18-1) dissolved in autoclaved tap water, sterilized, and provided as drinking water for 7 days. Before DSS treatment, *E. coli* colonization was tested by plating diluted fecal samples on MacConkey agar plates. After DSS treatment, the mice were either sacrificed or changed to normal drinking water and allowed to recover.

R-spondin overexpression in mice

Mice overexpressing R-spondin 3 have been previously described by Hilkens et al.³² These Rosa26Sor^{6(CAG - Rspo3)} animals were bred with Myh11-CreEr mice³³ to generate double-heterozygous Myh11-CreEr/Rosa26Sor^{6(CAG - Rspo3)} mice. To induce R-spondin 3 overexpression, tamoxifen (Sigma) was injected intraperitoneally at a single dose (4 mg/25 g body weight, diluted in 200 μ l corn oil) at the indicated time points before sacrifice.

Tissue processing

For paraffin embedding, the colon pieces were flushed with PBS and fixed in 2% PFA for 1 d. Paraffin embedding, sectioning, and H&E staining were performed by the Charité Core Unit Immunopathology for Experimental Models. To visualize the microbiota using FISH, feces-filled colon pieces were fixed in methanol-Carnoy fixative (60% (v/v) methanol, 30% (v/v) chloroform, and 10% (v/v) glacial acetic acid) for up to 3 weeks.

FISH

To visualize the microbiota, fixed tissue was processed according to a previously published protocol³⁴ For dehydration, tissue was washed twice in 100% methanol for 3 min, then twice in 100% ethanol for 20 min, followed by two 15-minute washes in 100% xylene before embedding in paraffin and sectioning. Tissue sections were rehydrated for 10 minutes by incubation in 100% xylene at 60°C, followed by 5 min in 100% ethanol. Slides were allowed to dry and overlaid with EUB388-Cy3 probe (Biomers, 1 µg/µl) in hybridization solution (20 mM Tris – HCl, pH 7.4, 0.9 M NaCl, 0.1% (w/v) SDS). A cover slide was used to prevent drying and slides were incubated at 50°C overnight in a humidified chamber. Slides were washed in PBS 3× for 5 min and blocked for 30 min before the primary antibody. Mouse anti-Muc2 serum (kindly provided by Gunnar Hansson) was added and incubated overnight. After an additional washing step, secondary antibody (anti-rabbit Alexa 488, anti-mouse Alexa 647) staining was performed for 2 h. The slides were washed 3 times in PBS and mounted.

Immunofluorescence

Paraffin-embedded sections were rehydrated and subjected to antigen retrieval and blocking, followed by incubation with primary antibodies against Ki67, E-cadherin, or γH2AX (for details, see Supplementary Table S1) overnight, followed by a washing step with PBS-Triton and incubation with secondary antibody for 1 h. For γH2AX, the secondary antibody was incubated overnight. After washing with PBS-Triton, the

samples were mounted to prevent fading. Samples were imaged using a Leica Sp8 confocal microscope.

Single-molecule RNA ISH hybridization

Sections of human colon tissue were processed for RNA in situ detection of R-spondin 3 using an RNAscope Red Detection Kit, according to the manufacturer's instructions (Advanced Cell Diagnostics, Hayward, CA, USA). Positive and negative control probes were used for each experiment according to the manufacturer's instructions. The probes used in this study are listed in Supplementary Table S3.

Quantitative RT-PCR

RNA was extracted from snap-frozen colon tissue using the RNeasy RNA Purification Kit (Qiagen) and on-column DNase digestion. qPCR was performed using a Power SYBR Green RNA-to-CT 1-Step Kit (Applied Biosystems), according to the manufacturer's instructions. Reactions were performed in 25 µl containing 50 ng RNA, 12.5 µl SYBR Green mix, 0.16 µl RT mix, and 0.2 µM primer (for sequences see Supplementary Table S4). Program: 30 min at 48°C, 10 min at 95°C, followed by 40 cycles of 15 s at 95°C/60 s at 60°C. For each oligonucleotide pair and RNA sample, the reaction was performed in triplicate. The amplification plots obtained from RT-PCR were analyzed using the StepOne ϕ Real-Time PCR Software v2.2. The expression levels of the target genes were normalized to those of glyceraldehyde-3-phosphate dehydrogenase in each sample.

Microarray analysis

For analysis of mice infected with WT M1/5 or $\Delta clbR$ *E. coli*, RNA from the colon was isolated using the RNeasy Mini Kit (Qiagen), as described above. Microarray experiments were performed as independent dual-color dye-reversal color-swap hybridizations using two biological replicates per group for the infected mice. Quality control and quantification of total RNA were carried out using an Agilent 2100

Bioanalyzer (Agilent Technologies) and a NanoDrop 1000 UV – Vis spectrophotometer (Kisker). RNA labeling was performed using a dual-color Quick-Amp Labeling Kit (Agilent Technologies). Briefly, mRNA was reverse transcribed and amplified using an oligo-dT-T7 promoter primer, and the resulting cRNA was labeled with cyanine 3-CTP or cyanine 5-CTP. After precipitation, purification, and quantification, 1.25 µg of each labeled cRNA was fragmented and hybridized to whole-genome mouse 4 × 44 K multipack microarrays (Agilent -014,868, whole mouse genome 4 × 44 K microarray kit) according to the manufacturer's protocol (Agilent Technologies). Microarray scanning was performed at 5 µm resolution using a G2565CA high-resolution laser microarray scanner (Agilent Technologies) with an extended dynamic range (XDR). Microarray image data were analyzed with image analysis/feature extraction software (G2567AA version A.11.5.1.1, Agilent Technologies) using default settings and the GE2_1105_Oct12 extraction protocol. Raw data was background-corrected and normalized using R package limma.³⁵ Microarray data have been deposited in the Gene Expression Omnibus (GEO; <https://www.ncbi.nlm.nih.gov/geo/>) of the National Center for Biotechnology Information under accession numbers GSE205403.

GSEA analysis

We performed GSEA on genes pre-ranked by gene expression-based t-score between colon epithelium isolated from WT *E. coli*-infected animals and $\Delta clbR$ mutant-infected animals using the fgsea R package with 5000 permutations. We used gene sets from MSigDB v7.1 and a gene set of a stem cell signature obtained from Lgr5+ cells in the intestinal crypts. P-values were adjusted for multiple testing using a global FDR according to the method described by Benjamini and Hochberg. The R version 4.1 was used and can be obtained from <https://cran.r-project.org/>, whereas the fgsea package can be retrieved from <https://www.bioconductor.org>. The computational code for the GSEA analysis of microarray data in this study can be accessed under https://github.com/Sigal-Lab/Harnack_pks_E.coli_barrier.

Statistics

No statistical methods were used to determine sample size. Mouse experiments were performed with at least $n = 3$ biological replicates, except for the microarray analysis, in which two biological replicates were used. No mice were excluded from the experiments. All data are presented as the mean \pm SD for the various groups. Statistics are based on 'n' biological replicates. Student's t-test was performed to compare two groups. All analyses of statistical significance were calculated and displayed compared to the reference control group unless otherwise stated. GraphPad Prism 7 software was used for data visualization and statistical analysis.

Author's contribution

CH and MS designed the study; CH performed most of the experiments and analyses; HB performed bioinformatics analysis of the transcriptome data; H-JM performed and analyzed the microarray; LL performed immunofluorescence staining and analysis; TS provided the mice. The MS was written by CH and MS, and all authors provided feedback.

Acknowledgments

We would like to thank Stefanie Müllerke and Janine Wolff for their excellent technical support, Uwe Klemm, Daniela Groine, Manuela Primke, and the members of the animal facility of the MPI for Infection Biology for their support with the management of the mouse colony, and Rike Zietlow for editing the paper. We also thank the members of the Sigal Lab for their constructive feedback.

Disclosure statement

No potential conflict of interest was reported by the author(s).

Funding

MS received funding from the DFG (Si 1983 3/1 and Si1983 4/1), European Research Council (ERC-Starting Grant REVERT) and the BMBF (PACE Therapy Consortium).

Data availability statement

Microarray data have been deposited in the gene expression omnibus (GEO; <https://www.ncbi.nlm.nih.gov/geo/>) of the National Center for Biotechnology Information under accession number GSE205403, reviewer token: sxcrkgounnorlmd.

References

- Nougayrede JP, Homburg S, Taieb F, Boury M, Brzuszkiewicz E, Gottschalk G, Buchrieser C, Hacker J, Dobrindt U, Oswald E. *Escherichia coli* induces DNA double-strand breaks in eukaryotic cells. *Science*. 2006;313(5788):848–851. doi:10.1126/science.1127059.
- Arthur JC, Perez-Chanona E, Mühlbauer M, Tomkovich S, Uronis JM, Fan T-J, Campbell BJ, Abujamel T, Dogan B, Rogers AB, et al. Intestinal inflammation targets cancer-inducing activity of the microbiota. *Science*. 2012;338(6103):120–123. doi:10.1126/science.1224820.
- Cougnoux A, Dalmaso G, Martinez R, Buc E, Delmas J, Gibold L, Sauvanet P, Darcha C, Déchelotte P, Bonnet M, et al. Bacterial genotoxin colibactin promotes colon tumour growth by inducing a senescence-associated secretory phenotype. *Gut*. 2014;63(12):1932–1942. doi:10.1136/gutjnl-2013-305257.
- Iftekhar A, Berger H, Bouznad N, Heuberger J, Boccellato F, Dobrindt U, Hermeking H, Sigal M, Meyer TF. Genomic aberrations after short-term exposure to colibactin-producing *E. coli* transform primary colon epithelial cells. *Nat Commun*. 2021;12(1):1003. doi:10.1038/s41467-021-21162-y.
- Pleguezuelos-Manzano C, Puschhof J, Rosendahl Huber A, van Hoeck A, Wood HM, Nomburg J, Gurjao C, Manders F, Dalmaso G, Stege PB, et al. Mutational signature in colorectal cancer caused by genotoxic pks(+) *E. coli*. *Nature*. 2020;580(7802):269–273. doi:10.1038/s41586-020-2080-8.
- Dziubanska-Kusibab PJ, Berger H, Battistini F, Bouwman BAM, Iftekhar A, Katainen R, Cajuso T, Crosetto N, Orozco M, Aaltonen LA, et al. Colibactin DNA-damage signature indicates mutational impact in colorectal cancer. *Nat Med*. 2020;26(7):1063–1069. doi:10.1038/s41591-020-0908-2.
- Hartl K, Sigal M. Microbe-driven genotoxicity in gastrointestinal carcinogenesis. *IJMS*. 2020;21(20):7439. doi:10.3390/ijms21207439.
- Lupp C, Robertson ML, Wickham ME, Sekirov I, Champion OL, Gaynor EC, Finlay B. Host-mediated inflammation disrupts the intestinal microbiota and promotes the overgrowth of Enterobacteriaceae. *Cell Host & Microbe*. 2007;2(3):204. doi:10.1016/j.chom.2007.08.002.
- Morgan XC, Tickle TL, Sokol H, Gevers D, Devaney KL, Ward DV, Reyes JA, Shah SA, LeLeiko N, Snapper SB, et al. Dysfunction of the intestinal microbiome in inflammatory bowel disease and treatment. *Genome Biol*. 2012;13(9):R79. doi:10.1186/gb-2012-13-9-r79.
- Petersen AM, Halkjaer SI, Gluud LL. Intestinal colonization with phylogenetic group B2 *Escherichia coli* related to inflammatory bowel disease: a systematic review and meta-analysis. *Scand J Gastroenterol*. 2015;50(10):1199–1207. doi:10.3109/00365521.2015.1028993.
- Cuevas-Ramos G, Petit CR, Marcq I, Boury M, Oswald E, Nougayrède J-P. *Escherichia coli* induces DNA damage in vivo and triggers genomic instability in mammalian cells. *Proc Natl Acad Sci USA*. 2010;107(25):11537–11542. doi:10.1073/pnas.1001261107.
- Stehr M, Greweling MC, Tischer S, Singh M, Blöcker H, Monner DA, Müller W. Charles river altered schaedler flora (CRASF[®]) remained stable for four years in a mouse colony housed in individually ventilated cages. *Lab Anim*. 2009;43(4):362–370. doi:10.1258/la.2009.0080075.
- Roy U, Gálvez EJC, Iljazovic A, Lesker TR, Błażejowski AJ, Pils MC, Heise U, Huber S, Flavell RA, Strowig T. Distinct microbial communities trigger colitis development upon intestinal barrier damage via innate or adaptive immune cells. *Cell Reports*. 2017;21(4):994–1008. doi:10.1016/j.celrep.2017.09.097.
- Thiemann S, Smit N, Roy U, Lesker TR, Gálvez EJC, Helmecke J, Basic M, Bleich A, Goodman AL, Kalinke U, et al. Enhancement of IFN γ production by distinct commensals ameliorates salmonella-induced disease. *Cell Host & Microbe*. 2017;21(6):682–694 e685. doi:10.1016/j.chom.2017.05.005.
- Chassaing B, Aitken JD, Malleshappa M, Vijay-Kumar M. Dextran sulfate sodium (DSS)-induced colitis in mice. *Curr Protoc Immunol*. 2014;104(25). doi:10.1002/0471142735.im1525s104. Unit 15.
- Wallenstein A, Rehm N, Brinkmann M, Selle M, Bossuet-Greif N, Sauer D, Bunk B, Spröer C, Wami HT, Homburg S, et al. Erratum for Wallenstein et al., “C1bR is the key transcriptional activator of colibactin gene expression in *Escherichia coli*”. *mSphere*. 2020;5(4). doi:10.1128/mSphere.00591-20.
- Haberman Y, Karns R, Dexheimer PJ, Schirmer M, Somekh J, Jurickova I, Braun T, Novak E, Bauman L, Collins MH, et al. Ulcerative colitis mucosal transcriptomes reveal mitochondriopathy and personalized mechanisms underlying disease severity and treatment response. *Nat Commun*. 2019;10(1). doi:10.1038/s41467-018-07841-3.
- Kaiko GE, Ryu SH, Koues OI, Collins PL, Solnica-Krezel L, Pearce EJ, Pearce EL, Oltz EM, Stappenbeck TS. The colonic crypt protects stem cells from microbiota-derived metabolites. *Cell*. 2016;165(7):1708–1720. doi:10.1016/j.cell.2016.05.018.
- Harnack C, Berger H, Antanaviciute A, Vidal R, Sauer S, Simmons A, Meyer TF, Sigal M. R-spondin 3 promotes stem cell recovery and epithelial regeneration in the colon. *Nat Commun*. 2019;10(1):4368. doi:10.1038/s41467-019-12349-5.
- Greicius G, Kabiri Z, Sigmundsson K, Liang C, Bunte R, Singh MK, Virshup DM. PDGFR α + pericyptal stromal cells are the critical source of Wnts and RSPO3 for murine intestinal stem cells in vivo. *Proc Natl Acad Sci USA*. 2018;115(14):E3173–E3181. doi:10.1073/pnas.1713510115.

21. Shivdasani RA, Clevers H, de Sauvage FJ. Tissue regeneration: Reserve or reverse? *Science*. 2021;371(6531):784–786. doi:10.1126/science.abb6848.
22. Swidsinski A, Ladhoff A, Perntaler A, Swidsinski S, Loening-Baucke V, Ortner M, Weber J, Hoffmann U, Schreiber S, Dietel M, et al. Mucosal flora in inflammatory bowel disease. *Gastroenterology*. 2002;122(1):44–54. doi:10.1053/gast.2002.30294.
23. Barker N, van Es JH, Kuipers J, Kujala P, van den Born M, Cozijnsen M, Haegebarth A, Korving J, Begthel H, Peters PJ, et al. Identification of stem cells in small intestine and colon by marker gene *Lgr5*. *Nature*. 2007;449(7165):1003–1007. doi:10.1038/nature06196.
24. Iftekhar A, Sigal M. Defence and adaptation mechanisms of the intestinal epithelium upon infection. *Int J Med Microbiol*. 2021;311(3):151486. doi:10.1016/j.ijmm.2021.151486.
25. Johansson ME, Phillipson M, Petersson J, Velcich A, Holm L, Hansson GC. The inner of the two Muc2 mucin-dependent mucus layers in colon is devoid of bacteria. *Proc Natl Acad Sci USA*. 2008;105(39):15064–15069. doi:10.1073/pnas.0803124105.
26. Litvak Y, Byndloss MX, Baumler AJ. Colonocyte metabolism shapes the gut microbiota. *Science*. 2018;362(6418):eaat9076. doi:10.1126/science.aat9076.
27. Litvak Y, Baumler AJ. Microbiota-nourishing immunity: a guide to understanding our microbial self. *Immunity*. 2019;51(2):214–224. doi:10.1016/j.immuni.2019.08.003.
28. Lopez CA, Miller BM, Rivera-Chavez F, Velazquez EM, Byndloss MX, Chavez-Arroyo A, Lokken KL, Tsois RM, Winter SE, Baumler AJ. Virulence factors enhance *Citrobacter rodentium* expansion through aerobic respiration. *Science*. 2016;353(6305):1249–1253. doi:10.1126/science.aag3042.
29. Papapietro O, Teatero S, Thanabalasuriar A, Yuki KE, Diez E, Zhu L, Kang E, Dhillon S, Muise AM, Durocher Y, et al. R-spondin 2 signalling mediates susceptibility to fatal infectious diarrhoea. *Nat Commun*. 2013;4(1):1898. doi:10.1038/ncomms2816.
30. Wehkamp J, Fellermann K, Herrlinger KR, Bevins CL, Stange EF. Mechanisms of disease: defensins in gastrointestinal diseases. *Nat Rev Gastroenterol Hepatol*. 2005;2(9):406–415. doi:10.1038/ncpgasthep0265.
31. Cox CB, Storm EE, Kapoor VN, Chavarria-Smith J, Lin DL, Wang L, Li Y, Kljavin N, Ota N, Bainbridge TW, et al. IL-1R1-dependent signaling coordinates epithelial regeneration in response to intestinal damage. *Sci Immunol*. 2021;6(59). doi:10.1126/sciimmunol.abe8856.
32. Hilkens J, Timmer NC, Boer M, Ikink GJ, Schewe M, Sacchetti A, Koppens MAJ, Song J-Y, Bakker ERM. RSPO3 expands intestinal stem cell and niche compartments and drives tumorigenesis. *Gut*. 2017;66(6):1095–1105. doi:10.1136/gutjnl-2016-311606.
33. Herring BP, Hoggatt AM, Burlak C, Offermanns S. Previously differentiated medial vascular smooth muscle cells contribute to neointima formation following vascular injury. *Vasc Cell*. 2014;6(1):21. doi:10.1186/2045-824X-6-21.
34. Earle KA, Billings G, Sigal M, Lichtman J, Hansson G, Elias J, Amieva M, Huang K, Sonnenburg J. Quantitative imaging of gut microbiota spatial organization. *Cell Host & Microbe*. 2015;18(4):478–488. doi:10.1016/j.chom.2015.09.002.
35. Ritchie ME, Phipson B, Wu D, Hu Y, Law CW, Shi W, Smyth GK. Limma powers differential expression analyses for RNA-sequencing and microarray studies. *Nucleic Acids Research*. 2015;43(7):e47. doi:10.1093/nar/gkv007.